

## TACTICAL LASER SYSTEMS PERFORMANCE ANALYSIS IN VARIOUS WEATHER CONDITIONS

Capt. R. Sabatini

Italian Air Force Research and Flight Test Division (DASRS) - Official Test Centre (RSV)

Technical Group (GT) - Avionics and Armament Evaluation Service (SSAA)

Pratica di Mare Airport

Pomezia 00040 (Rome), ITALY

### SUMMARY

A method for evaluating the performance of laser systems operating in the infra-red is presented in this paper. Particularly, state-of-the-art Nd :YAG target designators (LTD) performance are investigated in realistic operational scenarios, taking into account laser beam atmospheric propagation and target reflection characteristics, in different operational and environmental conditions.

Various standard atmospheric propagation models have been used for the 1.064  $\mu\text{m}$  wavelength of Nd :YAG and their results compared. Furthermore, a simplified laser beam propagation model has been developed taking into account both absorption and scattering effects, in various weather conditions (visibility, humidity, etc.). Particularly, the model for dry-air conditions has been derived from the studies and experiments conducted by Elder and Strong on infrared laser propagation at various wavelengths, while for rain propagation the basic model has been integrated with the equations developed by Middleton.

Moreover, an appropriate reflection model has been used and different geometric conditions taken into account, in order to evaluate the performance of laser systems in realistic operational scenarios.

The number of parameters in the models has been reduced in order to make the overall algorithm manageable in a PC mission planning program to be delivered at a Flying Squadron level, preserving an acceptable level of reliability for the operational and atmospheric conditions of practical interest.

All conclusions drawn here are referred to laser target designators, but they apply to most non-coherent detection laser systems including range finders and beam riders operating at 1.064  $\mu\text{m}$ .

### LIST OF SYMBOLS

$H_t$	MSL altitude of transmitter
$H_r$	MSL altitude of receiver
$H_g$	MSL altitude of target
$R_T$	range transmitter-target
$R_R$	range target-receiver
$\alpha$	aircraft angle of incidence
$\gamma$	aircraft ramp angle
$\gamma_r$	angle between the LOS target-receiver and the perpendicular to the aperture

$Q_d$	laser depression angle
$\varepsilon$	receiver depression angle
$\eta$	target inclination over the horizon
$Q_t$	angle between the LOS transmitter-target and the perpendicular to the target surface
$Q_r$	angle between LOS receiver-target and the perpendicular to the target surface
$MDP$	seeker minimum detectable power density
$\rho_T$	target reflectivity
$\Phi_o$	transmitter pick power
$D_R$	diameter of receiving aperture
$A$	illuminated area of target
$A_t$	area of target surface
$A_b$	beam area at a distance $R_T$
$V$	visibility
$w$	water vapour content
$w_t$	water vapour in the trans. path
$w_r$	water vapour content in the rec. path
$\rho$	relative humidity
$\tau_{ai}$	absorptive transmittance
$\tau_{asi}$	transmittance due to scattering
$\beta$	scattering coefficient
$\tau_{atm}$	atmospheric transmittance
$D_L$	beam diameter at transmitter
$\alpha_T$	beam divergence
$F$	energy density at target
$G$	irradiance of target surface
$U$	transmitted energy
$\sigma_w$	sea-level atmospheric attenuation coeff.
$\alpha_{HT}$	$\sigma_w$ fractional decrease from $H_t$ to sea level
$A_R$	receiver aperture area
$A_M$	projected spot area in the plane normal to the receiver sight line
$\beta_{HR}$	$\sigma_w$ fractional decrease from sea level to $H_r$

### INTRODUCTION

Technological development in the realm of optronics have led to innovative concepts in the mission management of current and next generation ground attack aircraft. Particularly, tactical laser systems including LIDAR, rangefinders (LRF) and target designators (LTD) are being used extensively today by most air forces in the world and new promising laser technologies are being explored. Most laser systems are active devices that operate in a manner very similar to microwave radars but at much higher frequency (e.g., LIDARS, LRF).

Other devices (e.g., LTD, Beam-riders) are simply used to precisely direct laser guided bombs (LGB) or other airborne weapons against ground targets. A combination of both functions is often encountered in modern integrated airborne navigation-attack systems.

Compared to similar microwave devices, the higher frequency of laser systems has the beneficial effect of smaller components and remarkable angular resolution values. On the other hand, laser systems performance are much more sensitive to the vagaries of the atmosphere and are thus generally restricted to shorter ranges in the lower atmosphere than microwave radar.

Because of the existence of atmospheric windows and the availability of suitable components (laser sources), laser systems are built at specific wavelengths. Most tactical laser systems are constructed at 1.064  $\mu\text{m}$  (Nd:YAG), 1.54  $\mu\text{m}$  (Er:glass and Raman-shifted Nd:YAG), and 10.6  $\mu\text{m}$  ( $\text{CO}_2$ ) wavelengths. Laser systems can be grouped according to the detection technique (i.e., coherent or non-coherent), the signal modulation technique, the type of measurement (if any), the wavelength of operation or the function performed. Generally, the term LIDAR (or LADAR) is referred to active devices belonging to the family of coherent detection laser systems. This paper, however, will concentrate on LTD/LGB combinations, which are typically included (together with most LRF) in the group of non-coherent detection laser systems. Since most state-of-the-art LTD/LGB combinations operate at 1.064  $\mu\text{m}$  wavelength (Nd:YAG), the laser beam atmospheric propagation and target reflection models have been optimised for this wavelength, taking also into account other characteristics of existing systems.

The theory of operation of laser weapon systems is simple. The LTD is an accurate pointing system which provides the laser source, the precision optics and stabilisation required to accurately shine the laser beam on the target. The LGB detector generate an electric signal when light is received at the wavelength of the laser, consequently the laser light reflecting off of the target is "visible" to the weapon. This provides signals on which the weapon can "home" toward the target by actuating its aerodynamic surfaces. Obviously, the pointing accuracy of the laser is most important, as any laser error will degrade the accuracy of the weapon.

Over the last decade, the Italian Air Force Research and Flight Test Establishment (DASRS-RSV) has been involved in various activities related with laser systems for airborne applications. Particularly, a Laser Designation Pod (LDP) with both TV and IR

capability has been integrated on the TORNADO aircraft, together LGB of various characteristics. Since the beginning of the activities, it appeared essential to define the most appropriate methods of LDP/LGB performance evaluation, in a representative part of the aircraft envelope and in realistic operational scenarios. This was important not only for experimental purposes, but also considering the remarkable advantage that the introduction of these methodologies could determine in the refinement of the tactics of employment of laser systems, in both training and attack missions.

Unfortunately, the available scientific and technical literature was not sufficient alone to allow such a deep investigation. Moreover, the majority of required technical data about the LTD/LGB systems were not made available by the manufacturers.

Therefore, the ItAF preceded autonomously, using the experience gained in flight test activities conducted at RSV and performing some laboratory measurements at DASRS in order to determine the LDP/LGB characteristics.

These activities permitted to obtain all information required for a PC mission planning program, that is now being implemented for delivery at an operational level. In perspective, developing an adequate display format, a similar program may even be used on the aircraft for real-time mission management.

The paper begins with a review of the underlying theory behind the algorithms used in the program. Particularly, a discussion about the laser range equation is presented, followed by a description of the atmospheric propagation/reflection models and of the relevant geometric elements of a typical attack mission. Successively, the practical applications of the study are discussed and the results of some calculations are presented relative to an example of LTD/LGB combination.

The paper closes with some concluding remarks. Three appendixes present more details about the mathematical derivation of the various equations and the curves describing in a graphic form the range performance of the particular LTD/LGB combination considered, in various weather conditions.

#### LASER RANGE EQUATION

A fundamental problem in laser systems analysis is the determination of the total optical power density that is present at the receiver aperture (case of LIDAR and LRF) or laser guided bomb (LGB) seeker and, consequently, the total optical power incident on the photosensitive element of the receiver (i.e., the detector).



beam propagation model has been developed for the 1.064  $\mu\text{m}$  wavelength of Nd:YAG laser. The model takes into account absorption and scattering effects and is valid for dry-air and rain conditions for any value of visibility and relative humidity. Particularly, the model for dry-air conditions has been derived from the studies and experiments conducted by Elder, Strong [3] and Langer [4] on infrared laser propagation at various wavelengths, while for rain propagation the basic model has been integrated with the equations developed by Middleton [5].

In the following, only a brief outline of the relevant equations is presented. More details are given at Appendix B.

The simplified equations for dry-air conditions, referred to the four cases of practical interest, are the following :

$$\text{Visibility} \geq 6 \text{ km}, w_r > w_t, w_r > w_l$$

$$\tau_{\text{rain}} = k_i^2 \left( \frac{w_l^2}{w_r w_t} \right)^{\beta} \cdot \left\{ \exp \left[ -\frac{391}{V} \cdot \left( \frac{\lambda_l}{0.55} \right)^{-(0.057 \cdot V + 1.029)} \cdot (R_t + R_r) \right] \right\} \quad (3)$$

$$\text{Visibility} \geq 6 \text{ km}, w_r > w_t, w_r < w_l$$

$$\tau_{\text{rain}} = k_i^2 \left( \frac{w_l}{w_r} \right)^{\beta} \cdot \left\{ \exp \left[ -A w_r^{1/2} - \frac{391}{V} \cdot \left( \frac{\lambda_l}{0.55} \right)^{-(0.057 \cdot V + 1.029)} \cdot (R_t + R_r) \right] \right\} \quad (4)$$

$$\text{Visibility} < 6 \text{ km}, w_r > w_t, w_r < w_l$$

$$\tau_{\text{rain}} = k_i^2 \left( \frac{w_l}{w_r} \right)^{\beta} \cdot \left\{ \exp \left[ -A w_r^{1/2} - \frac{391}{V} \cdot \left( \frac{\lambda_l}{0.55} \right)^{-(0.26 \cdot V^{1/3})} \cdot (R_t + R_r) \right] \right\} \quad (5)$$

$$\text{Visibility} < 6 \text{ km}, w_r > w_t, w_r > w_l$$

$$\tau_{\text{rain}} = k_i^2 \left( \frac{w_l^2}{w_r w_t} \right)^{\beta} \cdot \left\{ \exp \left[ -\frac{391}{V} \cdot \left( \frac{\lambda_l}{0.55} \right)^{-(0.26 \cdot V^{1/3})} \cdot (R_t + R_r) \right] \right\} \quad (6)$$

The equation for rain conditions, is the following :

$$\tau_{\text{rain-LTD}} = k_i^2 \left( \frac{w_l^2}{w_r w_t} \right)^{\beta} \cdot \left\{ \exp \left[ -\beta_{\text{rain}} (R_t + R_r) \right] \right\} \quad (7)$$

where the scattering coefficient with rain ( $\beta_{\text{rain}}$ ) is a function of the rainfall-rate ( $\Delta x/\Delta t$ ) and the dimension of the rain drops ( $\alpha$ ), as described at Appendix B.

### GEOMETRIC CONSIDERATIONS

There are three cosine factors in equations (1) and (2). They are related to the assumption of a "Lambertian" reflector (i.e., diffuse reflection of the laser signal laser signal incident on the target surface). It is essential, in order to determine the performance of an LTD/LGB combination during an attack, to take into account the variation of the angles  $\gamma_r$ ,  $Q_t$  and  $Q_r$  (Fig. 1).

On the other hand, in order to calculate the maximum range for effective illumination (MIR), it is important to determine the maximum values of these angles during an attack. Moreover, the angles  $\gamma_r$ ,  $Q_t$  and  $Q_r$  should be expressed as functions of other physical or geometrical parameters that are known prior the mission (e.g., seeker FOV, angle  $\eta$ , etc.).

From Eq. (2), the maximum theoretical value of the angle  $\gamma_r$  is :

$$\gamma_{r(MDP)} = \arccos \left( \frac{MDP \cdot \pi R_s^2}{\rho_r \Phi_s \cos \theta_t \cos \theta_r \tau_{\text{rain}}} \right) \quad (8)$$

However, we must consider that the seeker of the LGB must always intercept a portion of the reflected signal sufficient to activate the detector in order to guide the weapon against the target by appropriate motion of its control surfaces. In other words, as we can see in Fig. 2, the theoretical cone given by rotation of the angle  $\gamma_{r(MDP)}$  around the normal to the aperture, should always encompass the FOV of the seeker.

Therefore, since after the first laser pulse sequence is received  $\gamma_r$  should never exceed the FOV, we can reasonably assume that the maximum value of the angle  $\gamma_r$  is equivalent to the seeker FOV.

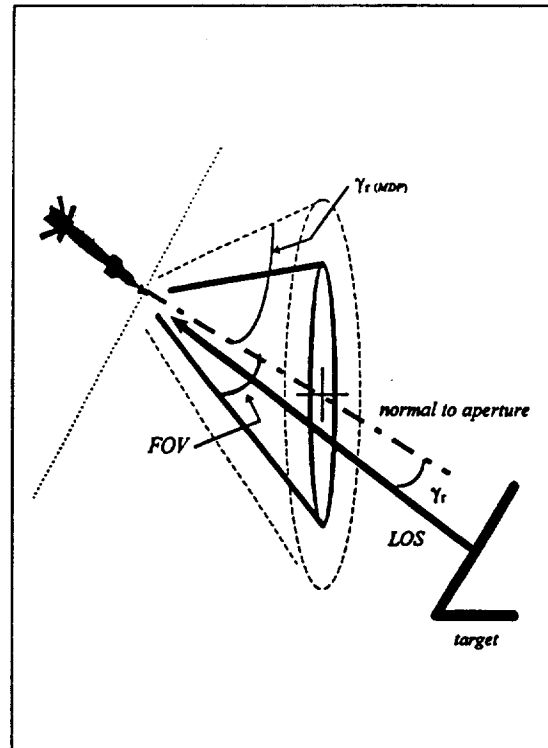


Figure 2. LGB-Target Geometry.

Considering the geometry of typical ground attack missions with LGB, also the the angles  $Q_t$  (angle between the LOS transmitter-target and the normal to the target surface) and  $Q_r$  (angle between the LOS receiver-target and the normal to the target surface), can be determined.

With reference to Fig. 1, the angles  $Q_i$  and  $Q_r$  can be expressed as :

$$Q_i = \eta + \varphi_i - 90^\circ \quad (9)$$

$$Q_r = 90^\circ - \eta - \varphi_r \quad (10)$$

where  $\eta$  is the target inclination,  $\varphi_i$  is the angle between the transmitted beam axis and the horizon ( $\varphi_i = Q_d - \gamma + \alpha$ ) and  $\varphi_r$  is the angle between the LGB-target LOS and the horizon ( $\varphi_r = \varphi_i - Q_i - Q_r$ ). Knowing  $Q_d$  (laser depression angle),  $\alpha$  and  $\gamma$ , it is possible to determine the value of the angle  $Q_i$  during the attack, solving the equation :

$$Q_i = \eta + Q_d - \gamma + \alpha - 90^\circ \quad (11)$$

More difficult is the determination of  $Q_r$ , since the angle  $\varphi_r$  can not be determined without knowing continuously the position assumed by the line of sight LGB-target (i.e., the guidance algorithms and accurate ballistics of the LGB). However, knowing the angle  $\beta$  at the beginning of the designation (from the ballistics of the unguided weapon) and taking  $\gamma_r$  equivalent to the seeker FOV, we have that :

$$\varphi_r = \beta \pm \gamma_{(MAX)} = \beta \pm FOV \quad (12)$$

Since, it is reasonable to assume that after the designation is initiated, the angle  $\gamma_r$  will be kept as low as possible by a PG-LGB, we can assume that  $\varphi_r = \beta$  in this case. Therefore, the approximate value of the angle  $Q_r$  during an attack with PG-LGB and BTB-LGB, can be determined solving the equations :

$$Q_r = 90 - \eta - \beta \quad \text{for PG-LGB} \quad (13)$$

$$Q_r = 90 - \eta - \beta + FOV \quad \text{for BTB-LGB} \quad (14)$$

For the purpose of determining the maximum values that the angles  $Q_i$  and  $Q_r$  can reach during an attack, which determine the absolute minimum performance of a particular LTD/LGB combination (worst case), it is meaningful to take into account the horizontal profile of a typical self-designation attack mission illustrated in Figure 3.

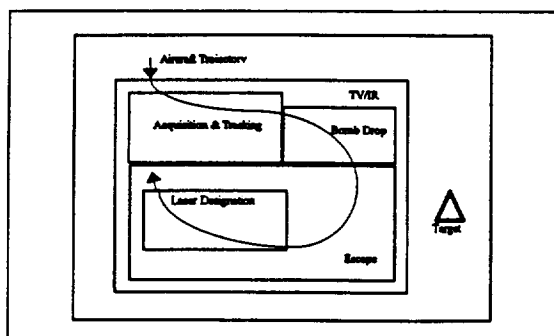


Figure 3. Mission horizontal profile (self-designation).

Since the designation is initiated in the final portion of the bomb drop trajectory, it is generally performed at a considerable range from the target (comparable to the visual range). This means that, normally, the angles  $Q_i$  and  $Q_r$  never reach values close to  $90^\circ$  during an attack, even in the worst case when  $\eta=90^\circ$ . On the other hand, in the case of horizontal target ( $\eta=0^\circ$ ), the cases where  $Q_i$  and  $Q_r$  get close to  $90^\circ$  are not of practical interest.

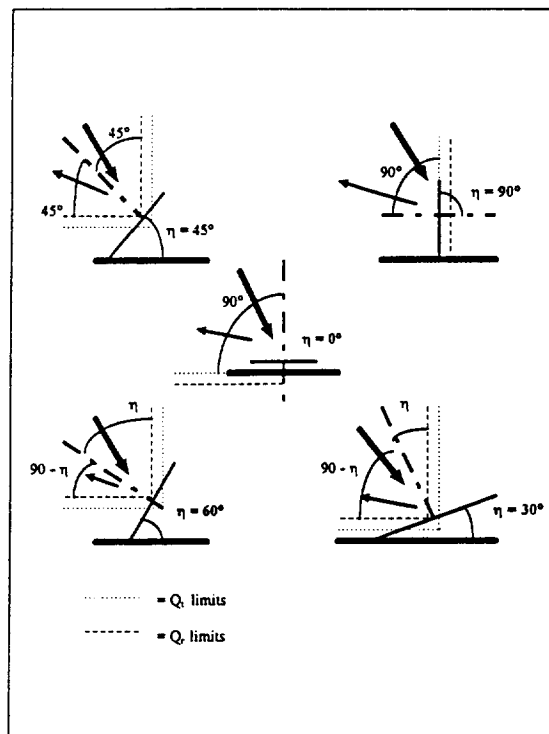


Figure 4.  $Q_i$  and  $Q_r$  limits.

Looking at Figure 4, it appears evident that the angle  $Q_i$  is smaller than  $\eta$  when  $\eta > 45^\circ$ , while it is generally smaller than the complementary of  $\eta$  when  $\eta < 45^\circ$ . Similar considerations apply for  $Q_r$ . Therefore, with these assumptions, the worst case conditions for  $Q_i$  and  $Q_r$  are the following :

$$\begin{cases} Q_{i(MAX)} = 90 - \eta \\ Q_{r(MAX)} = 90 - \eta \end{cases} \quad \text{for } \eta < 45^\circ$$

$$\begin{cases} Q_{i(MAX)} = \eta \\ Q_{r(MAX)} = \eta \end{cases} \quad \text{for } \eta \geq 45^\circ$$

## REFLECTIVITY CONSIDERATIONS

A surface that is a perfect diffuser scatters incident light equally in all directions. For such "ideal" surfaces, the intensity ( $W/m^2$ ) of diffuse reflected light is given by :

$$I_r = I_i k_r \cos \theta \quad 0 \leq \theta \leq \pi/2 \quad (15)$$

where  $I_i$  is the intensity of the light source at the target,  $\theta$  is the angle between the surface normal

and a line from the surface point to the light source (considered as a point source). The constant  $k_d$  is an approximation of the diffuse reflectivity, which depends on the nature of the material and the wavelength of the incident light.

Equation (15) can be written as the dot product of two unit vectors :

$$I_r = I_i k_d (L \cdot N) \quad (16)$$

where  $N$  is the surface normal and  $L$  the direction vector from the light source to the point on the surface.

The approximate diffuse reflectivity of various target materials ( $\lambda=1.064 \mu\text{m}$ ), are listed in Table 1.

Target	Material	Reflectivity
Shelter	Concrete (Aged)	40%
Metal Roof	Aluminum (Oxidized)	50%
Building Roof	Terra Cota	25%
Tanker	Steel (Painted)	30%
Aircraft	Painted Allum. Alloy	25%
Road	Asphalt	20%

TABLE 1. Diffuse Reflectivity of various targets.

In actuality, any reflection from a practical surface should be considered as the sum of a specular component and a diffuse component. The existence of these two components has been shown experimentally and is not a consequence of the choice of a particular model.

A surface attribute that is important to model is the surface roughness. A perfectly smooth surface reflects incident radiation in a single direction. A rough surface tends to scatter incident radiation in every direction, although certain directions may contain more reflected energy than others. This behaviour is obviously also dependent on the wavelength of radiation; a surface that is smooth for certain wavelengths may be rough for others. For example, oxidised or unpolished metal is smooth for radio waves (say  $\lambda=10^2$  m) and very rough for radiation in the near-infrared (NIR) part of the spectrum. In general, metals can be prevalently diffuse or specular reflectors in the NIR depending on whether they are polished or not. So reflection is not predominantly dependent on the material but also on its surface properties. Another factor in reflection is the grazing angle of the incident laser source. This can in fact determine the entity of the reflected signal and which component of reflection (i.e., diffuse or specular) is prevailing.

Therefore, a "realistic" reflection model should at least represent the target surface as some combination of a perfect diffuse reflector and a perfect specular surface. One such a model is described at Appendix C.

## CALCULATIONS

We can not attempt to calculate the range performance of a particular LTD/LGB combination, using the data given in Table 2. These data are referred to generic LTD and LGB systems operating at a wavelength of  $1.064 \mu\text{m}$ .

Using the equations described above, we can now calculate the range performance of this particular LTD/LGB combination in a certain operational scenario, with different atmospheric conditions (i.e., visibility, humidity, etc.).

<i>LTD</i>	
Beam Diameter	50 mm
Beam Divergence	0.5 mrad
Wavelength	1.064 $\mu\text{m}$
Pick Energy	120 mJ
Pulse Duration	20 nsec
<i>LGB</i>	
FOV	20°
MDP	3 $\mu\text{W}/\text{m}^2$

TABLE 2. LTD/LGB Characteristics

Moreover, with the same atmospheric conditions, we can calculate the performance of the systems when used against different targets (i.e., reflectivity, inclination), and the maximum distance of the illuminating aircraft for an effective designation.

The curves shown at Appendix C describe in a graphic form the range performance of the considered LTD/LGB combination, with different values of visibility (i.e., all other parameters have been set to the "worst case" value). Particularly, the range LTD-target is given as a function of the range LGB-target. The curves have been traced for different inclinations of the target over the horizon (i.e., different values of the angles  $Q_{i(MAX)}$  and  $Q_{r(MAX)}$ ).

Using these curves it is also possible to determine whether or not the attack can be performed with a certain estimated minimum illumination time.

Given the bomb initial conditions (i.e., velocity and trajectory, from the unguided weapon ballistics) before designation is initiated, it is possible to estimate the designation time, taking into account the time required by the LGB from those initial conditions to stabilise towards the target (i.e., guided weapon ballistics).

If the guidance algorithms are unknown it is possible to roughly estimate the designation time by assuming a straight trajectory of the bomb towards the target and a velocity in the final portion of its drop correspondent to the maximum theoretical velocity of the weapon. With these assumptions, the minimum theoretical range LGB-target before designation can be plotted in the graphs given at Appendix D and consequently the maximum range of the aircraft at the beginning of the designation is determined. Obviously, when this range is less than the Target Lethal Range (TLR), the attack can not be performed successfully.

For instance, assuming a maximum theoretical velocity of the LGB in the order of 800 fts/sec and a minimum designation time of 12 sec, the distance LGB-target before designation should not exceed 3 km, for an effective guidance. Plotting this value in the graphs D-1 and D-2, we notice that in the worst geometric conditions (i.e.,  $\eta$  close to  $0^\circ$  and  $90^\circ$ ) the range aircraft-target at the beginning of the designation is below the visual range (i.e., less than 1 km for a 2 km visibility and about 3 km for a 4 km visibility). In all other cases (i.e.,  $V > 4$  km) the illumination can be performed from a distance comparable to (or, theoretically, even greater than) the visual range.

#### APPLICATIONS OF THE STUDY

The equations presented in this paper can be used for estimation of LRF and LTD/LGB performance in different operational scenarios. Particularly, they can be the basis of a PC program for mission planning and optimisation, allowing validation and refinement of the operational tactics (for both self-designation and co-operative attacks). Moreover, adopting an adequate display format, they can be even used to implement a software for real-time mission management in the aircraft.

A possible display format for the PC Mission Planning Program (MPP) is shown in Figure 5.

The Maximum Illumination Range (MIR) circles should always encompass the Target Lethal Range (TLR) circle. The MIR at the beginning ( $MIR_1$ ) and at the end ( $MIR_2$ ) of the designation can be displayed (all other MIR circles are included between these two).

Knowing the target surface orientation, reflectivity and inclination, it is also possible to determine the optimal illumination sector (OIS) and the optimal bomb direction (OBD).

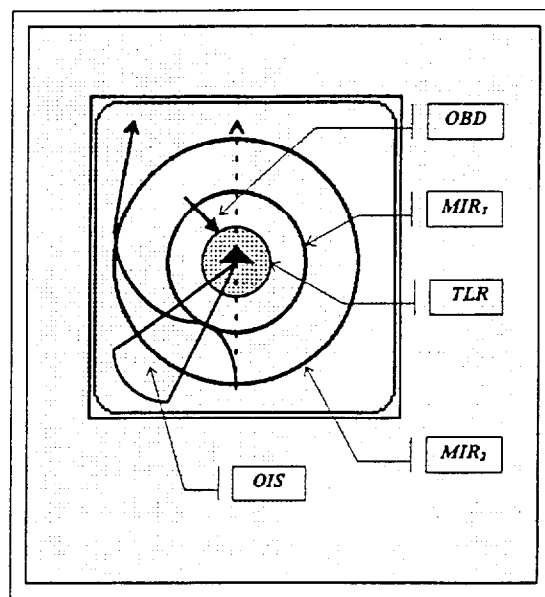


Figure 5. Possible MPP Display Format.

In order to obtain this kind of presentation, the operator should insert the following information :

- LDP characteristics
- LGB seeker MDP ;
- LGB seeker FOV
- Target surface reflectivity ;
- Target surface inclination ;
- Target surface orientation
- Visibility ;
- Relative humidity ;
- Temperature
- Expected bomb direction ;
- Desired Escape Direction.

A pictorial representation of a possible cockpit display format is shown in Figure 6.

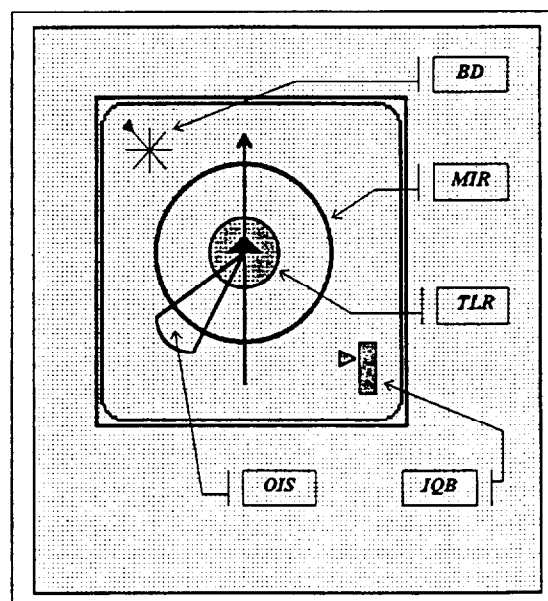


Figure 6. Possible Cockpit Display Format.

An indication of the MIR associated with current direction and position can be provided in real-time, together with an Illumination Quality Bar (IQB). Moreover, knowing the Bomb Direction (BD), it is possible to provide an indication of the OIS, including the MIR relative to it. In order to obtain this kind of presentation, assuming that all information required on relevant LDP and LGB types are available to the aircraft computer (together with aircraft-target relative position information), the pilot should insert prior the attack (e.g., through a dedicated data entry format), the following information :

- Type of LDP/LGB combination ;
- Target surface reflectivity ;
- Target inclination ;
- Visibility ;
- Relative humidity ;
- Temperature ;
- Expected bomb direction ;
- Target surface orientation.

The atmospheric parameters (i.e., visibility and humidity) should be obviously referred to the target location. If the relative humidity is unknown, it can be set to 100% (i.e., worst case). Similarly, if the target inclination is unknown or the target is a curve surface (e.g., a shelter) the inclination can be set to the worst case value (i.e., 90° or 0°).

#### FINAL REMARKS

In this paper we have illustrates the results of a study conducted by the Italian Air Force Research and Flight Test Establishment (DASRS-RSV) in order to define a method for predicting the performance of laser systems operating in the infrared, with different operational and environmental conditions.

The study was mainly addressed to airborne laser systems for target designation (LTD), used to precisely direct laser guided bombs (LGB) against ground targets. However, most of the results presented in this paper are applicable to all non-coherent detection laser systems (e.g., range finders, beam-riders, etc.).

An atmospheric laser beam propagation model has been implemented taking into account both absorption and scattering effects, in different weather conditions (visibility, humidity, etc.). The number of parameters in the model has been reduced as much as possible, in order to make the model manageable at an operational level, notwithstanding the model reliability for the atmospheric propagation window of interest. Moreover, an appropriate reflection model has been used and different geometric conditions taken into account, in order to evaluate the performance of the laser systems in realistic operational scenarios.

The results of the study are very encouraging, giving the opportunity to improve the tactics of employment of the laser guided weapons and to determine the range of possible uses of particular combinations LTD/LGB in favourable and adverse weather conditions.

An activity now ongoing is the implementation of a MPP, based on the algorithms developed in the study, for laser attack mission planning and optimisation at a Squadron level. It is expected that the software will also be able to assist in the definition of laser safety criteria for both test range and training operations.

Moreover, adopting an adequate display format, the algorithms developed can be even used to implement a software for real-time mission management in the aircraft.

#### ACKNOWLEDGMENT

The author gracefully acknowledge the valuable advise given by Lt.Col G Arpaia, Maj P Cuppone and Maj F Guercio of DASRS-RSV and the conversations held with Mr F Fouchard of Thomson Avionique (Paris).

#### REFERENCES

1. A. V. Jelalian. "Infrared laser radar system". AGARD CP482. Dec 1990.
2. R. D. Hudson. "Laser and low light television". Hughes Aircraft Company, CA, 1980.
3. T. Elder, J. Strong. "The infrared transmission of atmospheric windows". J. Franklin Ins., 1953.
4. R. M. Langer. Signal Corps Report No. DA-36-039-SC-72351. May 1957.
5. W. E. K. Middleton. "Vision through the atmosphere". Univ. of Toronto Press. 1952.
6. B. T. Phong. "An empirical model of light reflection". Journal of Applied Physics. 1975.

#### APPENDIX A

The beam area at a distance  $R_T$  is given by :

$$A_t = \frac{\pi(D_t + \alpha_r R_t)^2}{4} \quad (\text{A-1})$$

The energy density ( $J/m^2$ ) at the target as a function of transmitted energy is given by :

$$F = \frac{U}{A_t} e^{-(\alpha_a + \alpha_s R_t)} \quad (\text{A-2})$$

This energy density is measured normally to the transmitter line of sight (LOS).



Using equation (A-1), the equation (A-2) can be written in the form :

$$F = \frac{4U}{\pi(D_i + \alpha_r R_r)^2} e^{-(\sigma_a A_s)} \quad (\text{A-3})$$

The energy (G) of a laser spot that will irradiate a given target surface (A) is that portion passing through the projected area ( $A_N$ ) in the plane orthogonal to the sight line. The irradiance of the target surface can be calculated using the equation :

$$G = F \frac{A_N}{A} \quad (\text{A-4})$$

therefore :

$$G = \frac{4UA_N}{A\pi(D_i + \alpha_r R_r)^2} e^{-(\sigma_a A_s)} \quad (\text{A-5})$$

Assuming that the target surface ( $A_t$ ) is greater than the laser spot on target, we have :

$$A_N = A \cos \theta \quad (\text{A-6})$$

Therefore, in this case:

$$G = \cos \theta \frac{4UA_t}{A\pi(D_i + \alpha_r R_r)^2} e^{-(\sigma_a A_s)} \quad (\text{A-7})$$

A rigorous approach requires that all possible target-spot relative dimensions are taken into account (i.e., "extended" target, target smaller than laser spot and "wire" target). However, considering the aim of this paper, only the extended target case will be considered. In fact, for a typical airborne LTD the illuminated area of the target is smaller than 3 m<sup>2</sup> when the system is operated from a distance of 10 km. However, since the other cases are applicable to LRF (and other systems), a detailed explanation of them can be found in the literature [1], [2].

The brightness of the irradiated target is determined by the irradiance level and by the reflectance characteristics of the target surface with respect to wavelength. Assuming a Lambertian target (i.e., diffuse reflector), the brightness (B) is given by :

$$B = \frac{\rho_r G}{\pi} \quad (\text{A-8})$$

where  $\rho_r$  is the target diffuse reflectivity.

The energy ( $E_R$ ) collected by a receiving aperture observing this target is obtained from :

$$E_R = \frac{BA_r A_M}{R_r^2} e^{-(\sigma_a A_s)} \quad (\text{A-9})$$

$A_M$  is related to the target laser spot area by :

$$A_M = A \cos \theta \quad (\text{A-10})$$

Therefore, the final expression for energy intensity (I) at the receiver aperture for the Lambertian target

is, by substitution :

$$I = \frac{E_R}{A_r} = \frac{4\rho_r UA \cos \theta_i \cos \theta_r e^{-[\sigma_a (A_s + \beta_s R_s)]}}{\pi^2 (D_i + \alpha_r R_r)^2 R_r^2} \quad (\text{A-11})$$

Since  $A = A_b$  for an extended target (i.e., provided the entire spot is on the target), we have :

$$I = \frac{\rho_r U \cos \theta_i \cos \theta_r e^{-[\sigma_a (A_s + \beta_s R_s)]}}{\pi R_r^2} \quad (\text{A-12})$$

If the seeker of the "smart bomb" is not turned towards the target, an additional cosine factor would be introduced reducing the effective receiving aperture as a function of the angle between the line of sight and normal to the aperture ( $\gamma_R$ ). Therefore :

$$I = \frac{\rho_r U \cos \theta_i \cos \theta_r \cos \gamma_R e^{-[\sigma_a (A_s + \beta_s R_s)]}}{\pi R_r^2} \quad (\text{A-13})$$

If the transmitter and receiver are collocated (case of LRF), the equations can be simplified by setting :

$$\begin{aligned} H_r &= H_t & \beta_{HR} &= \beta_{HT} & \gamma_r &= 0 \\ R_r &= R_t = R_o & \alpha_r &= \alpha_t \end{aligned}$$

Therefore :

$$I = \frac{\rho_r U \cos^2 \theta_i e^{-[\sigma_a (A_s + \beta_s R_s)]}}{\pi R_o^2} \quad (\text{A-14})$$

## APPENDIX B

Attenuation of laser radiation in the atmosphere is described by the Beer's law :

$$\tau = I(z) / I_o = \exp(-\alpha z) \quad (\text{B-1})$$

where  $\tau$  is the transmittance,  $I_o$  is the transmitted energy,  $I(z)$  is the energy received at a distance  $z$  from the laser source and  $\sigma$  is the attenuation coefficient. If the attenuation coefficient is a function of the path, then Eq. (B-1) becomes :

$$\tau = \exp\left[-\int_0^z \sigma(z) dz\right] \quad (\text{B-2})$$

The attenuation coefficient is determined by four individual processes: molecular absorption, molecular scattering, aerosol absorption and aerosol scattering. Therefore, the atmospheric attenuation coefficient ( $\sigma$ ) is given by :

$$\sigma = \alpha + \beta \quad (\text{B-3})$$

where  $\alpha = \alpha_m + \alpha_a$  is the absorption coefficient and  $\beta = \beta_m + \beta_a$  is the scattering coefficient (the subscripts  $m$  and  $a$  designate the molecular and aerosol processes respectively). Each coefficient depends on the wavelength of the laser radiation.

A simple approach, yielding approximate values of the absorption coefficient has been suggested by Elder and Strong [3] and modified by Langer [4]. Their approach is particularly useful because it

provides a means of relating the atmospheric absorption of the *i*th window to the relative humidity (a readily measurable parameter).

The empirical expressions developed by Langer are:

$$\tau_a = \exp(-A_i \cdot w^{1/2}), \quad \text{for } w < w_i \quad (B-4)$$

$$\tau_a = k_i \left(\frac{w_i}{w}\right)^A \exp(-A_i \cdot w^{1/2}), \quad \text{for } w > w_i \quad (B-5)$$

where  $A_i$ ,  $k_i$ ,  $\beta_i$  and  $w_i$  are constants whose values are the listed in Tab. B-1,  $w$  (the total precipitable water in mm), is given by :

$$w = 10^{-3} z \rho_a \quad (B-6)$$

and  $\rho_a$  is the absolute humidity in  $g/m^3$ .

Window	$\Delta\lambda$ (nm)	$A_i$	$k_i$	$\beta_i$	$w_i$
I	0.72 - 0.94	0.0305	0.800	0.112	54
II	0.94 - 1.13	0.0363	0.765	0.134	54
III	1.13 - 1.38	0.1303	0.830	0.093	2.0
IV	1.38 - 1.90	0.211	0.802	0.111	1.1
V	1.90 - 2.70	0.350	0.814	0.1035	0.35
VI	2.70 - 4.30	0.373	0.827	0.095	0.26
VII	4.30 - 6.0	0.598	0.784	0.122	0.165

TABLE B-1. Constants for equations (B-4) and (B-5).

The value of  $\rho_a$ , the density of water vapour, can be found by multiplying the appropriate number in Table B-2 by the relative humidity.

Temperature										
°C	0	1	2	3	4	5	6	7	8	9
-20	0.89	0.81	0.74	0.67	0.61	0.56				
-10	2.15	1.98	1.81	1.66	1.52	1.40	1.28	1.18	1.08	0.98
0	4.84	4.47	4.13	3.81	3.52	3.24	2.99	2.75	2.54	2.34
10	9.33	8.94	8.57	8.22	7.89	7.57	7.27	6.99	6.73	6.48
20	17.22	16.84	16.48	16.14	15.81	15.50	15.20	14.92	14.65	14.39
30	30.04	29.67	29.31	28.97	28.64	28.32	28.01	27.71	27.42	27.14

TABLE B-2. Mass of water vapour in saturated air ( $g/m^3$ )

For instance, if the temperature is 24°C and the relative humidity is 75%, the absolute humidity is 16.2  $g/m^3$  and the precipitable water content is  $1.62 \times 10^{-2}$  mm per meter of path length.

Approximate values of the transmittance due to scattering ( $\tau_a$ ) can be obtained with the expression :

$$\tau_a = \exp \left[ - \frac{3.91}{V} \cdot \left( \frac{\lambda_i}{0.55} \right)^{-r} \cdot z \right] \quad (B-7)$$

where  $\lambda_i$  must be expressed in microns. For ranges between 6 and 100 km, the following linear regression can be used to calculate the

approximate values of  $\delta$  :

$$\delta = 0.0057 \times V + 1.025 \quad (B-8)$$

If, because of haze, the visual range is less than 6 km, the exponent  $\delta$  is related to the visual range by the following empirical formula :

$$\delta = 0.585 \times V^{1/3} \quad (B-9)$$

where  $V$  is in kilometres. For exceptionally good visibility  $\delta = 1.6$ , and for average visibility  $\delta \cong 1.3$ . The scattering coefficient with rain ( $\beta_{rain}$ ) is strongly dependent on the size of the drops. Middleton [5] has shown that  $\beta_{rain}$  is :

$$\beta_{rain} (cm^{-1}) = 1.25 \times 10^{-6} \times \frac{(\Delta x / \Delta t)}{a^3} \quad (B-10)$$

where  $\Delta x / \Delta t$  is the rainfall rate in cm/sec and  $a$  is the radius of the drops in cm.

Rainfall rates for four different rain conditions and the corresponding transmittance due to scattering of a 1.8 km path are shown in Table B-3.

Condition	Rainfall-rate (cm/hr)	$\tau_a$ for $z=1.8$ km
Light Rain	0.25	0.88
Medium Rain	1.25	0.74
Heavy Rain	2.5	0.65
Cloudburst	10.0	0.38

TABLE B-3.  $\tau_a$  of a 1.8 km path through rain.

### APPENDIX C

A reflection model commonly used in engineering applications where light/object interactions have to be described, is the Phong's model. This divides the reflectivity into a diffuse component and a specular component. The bi-directional spectral reflectivity is given by :

$$\rho_i(\lambda, \theta_r, \phi_r, \theta_i, \phi_i) = k_{diffuse} + k_{specular} \cos^n \phi \quad (C-1)$$

where  $k_{diffuse}$  is the fraction of energy diffusely reflected,  $k_{specular}$  is the fraction specularly reflected and  $\phi$  is the angle between the mirror direction  $R$  and the viewing direction  $V$  (Figure 5).

In his original paper [6], Phong gives :

$$k_{specular} = W(i) \quad (C-2)$$

implying a dependence on the incidence angle  $i$ . However, no details are given on the nature of  $W(i)$  and most implementations now ignore this and reduce the bidirectional reflectivity to a reflectivity that depends only on the outgoing angle of interest :

$$\rho_i(\lambda, \theta_r, \phi_r, \theta_i, \phi_i) = \rho_i(\lambda, \phi) \quad (C-3)$$

where the material is assumed to be isotropic.

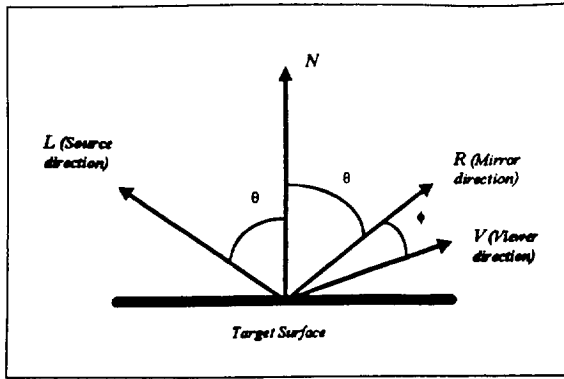


Figure 5. Vectors used in Phong reflection model.

Although there is nothing to prevent an anisotropic dependence of reflectivity on both the outgoing angles the Phong model is most often implemented as above. The empirical spread of the highlight about the mirror direction was Phong's important innovation, giving a cheap but effective way of calculating the geometry of the specular highlight. The Phong's model can be given in terms of the unit vectors associated with the geometry of the point under consideration. Therefore, for the reflected light intensity, we have :

$$I = I_s [k_s (\cos \theta) + k_r (\cos^2 \phi)] \quad (C-4)$$

or :

$$I = I_s [k_s (L \cdot N) + k_r (R \cdot V)^n] \quad (C-5)$$

where  $k_s$  is the specular reflection coefficient, usually taken to be a material dependent constant,  $n$  is the index that controls the "tightness" of the highlight.

Figure 6 shows the variation in light intensity at a point  $P$  on a surface calculated using equation (C-5). The intensity variation is shown as a profile (i.e., a function of the orientation of  $V$ ). The intensity at  $P$  is given by the length of  $V$  from  $P$  to its intersection with the profile. The semicircular part of the profile is the contribution from the diffuse and ambient terms. The specular part of the profile is shown for different values of  $n$ . Note that large values of  $n$  are required for a tight highlight to be obtained.

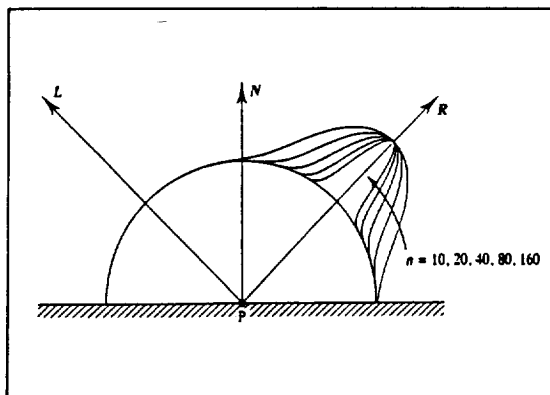


Figure 6. Intensity at P as a function of V orientation.

Another important factor, to be accounted for during daytime operation, is the sunlight reflected from the target. Particularly, the solar irradiance of the target ( $I_s$ ) at the operation wavelength plays an important role, since it adds to the  $I$  term in equation (C-4) to determine the amount of energy effectively received, after propagation, at the observer location.

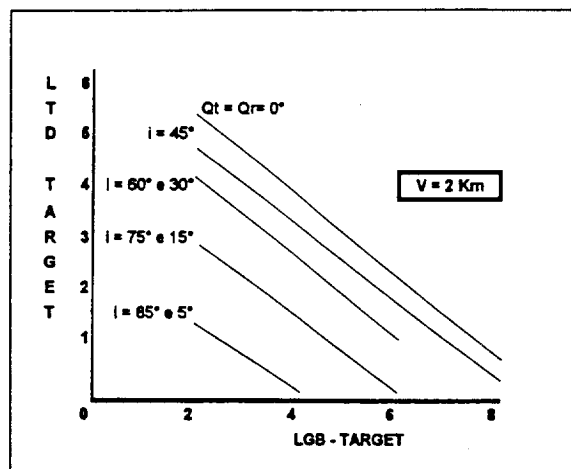
According to the Phong model (i.e., assuming a point source, a point observer and a point target), the intensity of reflected solar light at the wavelength considered can be approximated by :

$$I_r = E_s [k_s (\cos \theta) + k_r (\cos^2 \phi)] \quad (C-6)$$

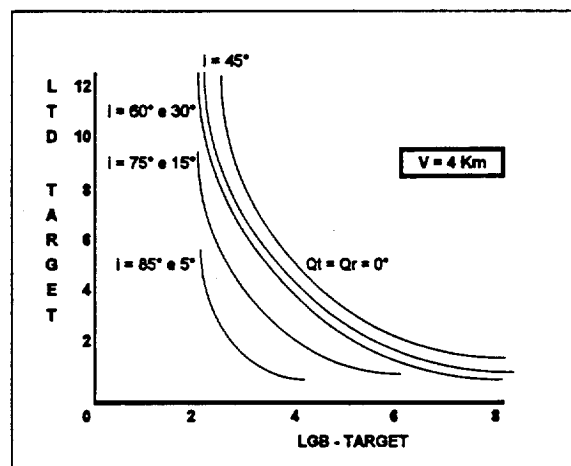
where  $E_s$  is the solar spectral irradiance at the target ( $W/m^2$ ) at the operating wavelength of the laser and  $\theta'$  is the angle between the solar illumination and the normal to the reflecting surface of the target.

APPENDIX D

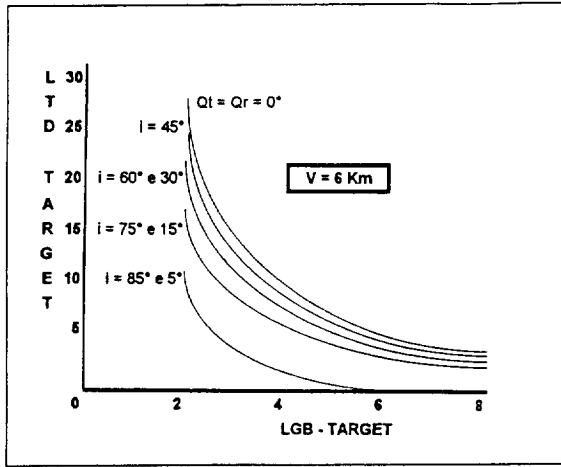
D-1



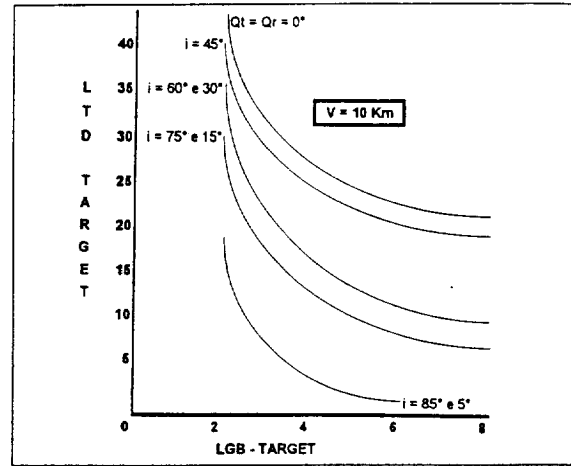
D-2



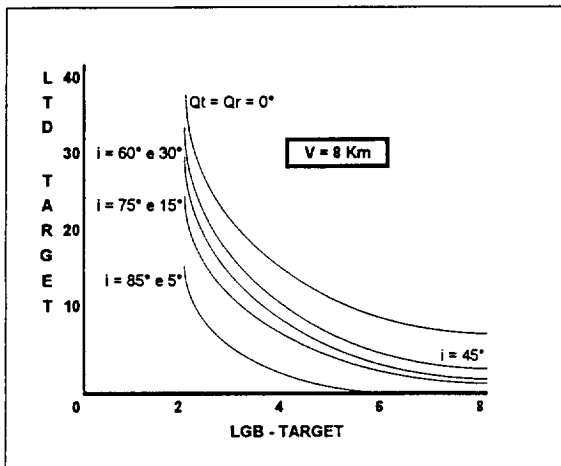
D-3



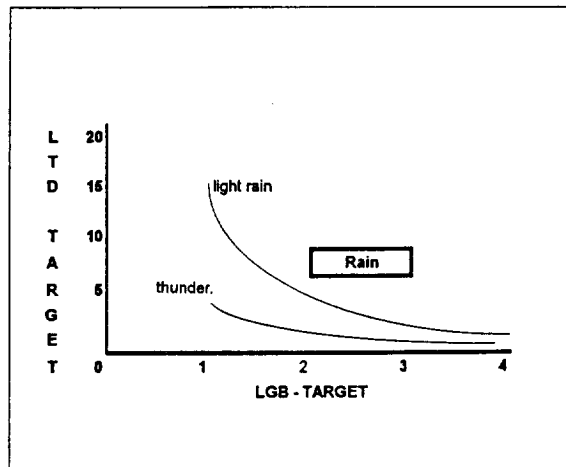
D-5



D-4



D-6



PAPER No.: 29

DISCUSSOR'S NAME: A.M. Bouchardy

COMMENT/QUESTION:

What type of accuracy do you need for input meteorological data to make good performance predictions?

AUTHOR/PRESENTER'S REPLY:

The model needs flying squadron level accuracy data (visibility and humidity provided by the airport meteorological office). Since the program is used for mission planning/optimisation a "worst case" approach is often acceptable.

PAPER No. 29

DISCUSSOR'S NAME: E. Schweicher

COMMENT/QUESTION:

1. Is the YAG laser diode-pumped or flash lamp pumped?
2. I found your value of 0.5 mrad a little bit too high for the laser divergence. Your comments?
3. How do you cope with the boresight problem between observation channel and designation channel?

AUTHOR/PRESENTER'S REPLY:

1. Flash lamp pumping.
2. The actual value is much smaller.
3. With a pilot/navigator commanded boresight facility. In single-seat aircraft (e.g. EF2000, AMX) an automatic boresight capability is highly desirable.

